

Wandering of a contact line at thermal equilibrium

Anusha Hazareesing and Marc Mézard

Laboratoire de Physique Théorique de l'École Normale Supérieure, 24 rue Lhomond, 75231 Paris Cedex 05, France

(Received 8 July 1998)

We reconsider the problem of the solid-liquid-vapor contact-line on a disordered substrate, in the collective pinning regime. We perform a replica variational calculation which confirms the scaling behavior obtained from Larkin-Imry-Ma-like arguments and provides a quantitative prediction for the correlation function of the line. This prediction is in good agreement with experimental findings for the case of superfluid helium on a caesium substrate. [S1063-651X(99)06307-2]

PACS number(s): 05.40.-q, 68.45.-v

I. INTRODUCTION

When a liquid partially wets a solid, the liquid-vapor interface terminates on the solid, at the contact line. If the solid surface is smooth, then at equilibrium we expect no distortions of the contact line, and Young's relation [1] giving the contact angle in terms of the interfacial tensions holds, that is

$$\gamma_{sv} - \gamma_{sl} = \gamma \cos(\theta_{eq}), \quad (1)$$

where $\gamma = \gamma_{lv}$.

We consider a case where the substrate is weakly heterogeneous and where the heterogeneities are "wetable" defects, leading to a space dependence of the interfacial tensions γ_{sv} and γ_{sl} . Favored configurations are those where the liquid can spread on a maximum number of defects. We thus expect distortions of the contact line which tends to be pinned by the defects. Moreover, the energy due to the liquid-vapor interface induces an elastic energy of the line. The competition between the elastic energy and the pinning due to the disorder gives rise to a nontrivial wandering of the line, a typical example of the general problem of manifolds in random media [2,3]. The case of the contact line is of special interest for several reasons. There exists by now good experimental data for the correlations which characterize the wandering of the line [4]. On the theoretical side, the problem presents two specific features. The elasticity of the line is due to the liquid-vapor interface and is therefore nonlocal. The pinning energy due to the surface heterogeneities is, up to a constant, a sum of local energy contributions due to the wetted defects. It has therefore nonlocal correlations which are of the "random field" type in the usual nomenclature of manifolds in random media.

In this paper we will consider the case of collective pinning where the strength of the individual pinning sites is small, but pinning occurs due to a collective effect. This seems to be the relevant situation for the experiments. The case of strong pinning by individual impurities was studied by Joanny and De Gennes [5]. Collective pinning is a particularly interesting phenomenon since the balance between the elastic energy and the pinning one results in the existence of a special length scale ξ , first discussed by Larkin in the context of vortex lines in superconductors [6]. This Larkin length is such that the lateral wandering of a line, thermalized at low temperatures, on length scales smaller than ξ , is

less than the correlation length Δ of the disorder (range of the impurities), while beyond ξ the lateral fluctuations become larger than Δ and the line probes different impurities. The Larkin length scale diverges in the limit where the strength of disorder goes to zero. At zero temperature, the line has a single equilibrium position when its length is smaller than ξ , while metastable states appear only for lengths larger than ξ . Therefore, one can think of the contact line, qualitatively, as an object which is rigid on small length scales (less than ξ) and fluctuates on larger length scales. A third length scale, which is relevant for the discussion, is the capillary length L_c , which is the length scale beyond which effects due to gravity become important: the line then becomes "flat" in the sense that its fluctuations do not grow any longer with the distance.

The collective pinning of the contact line was first addressed by Vannimenus and Pomeau [7]. They considered the case of very weak disorder in which the Larkin length ξ is larger than the capillary length. So their analysis only probes the "Larkin regime" of length scales less than ξ , in which there exist only very few metastable states. A more complete qualitative picture, making clear the role of ξ , can be obtained by some scaling arguments originally developed for some related problems by Larkin [6] and Imry-Ma [8]. For the case of the contact line, these arguments were introduced by Huse [10] and developed by De Gennes [1] and by Joanny and Robbins [9]. They lead to interesting predictions concerning the growth of lateral fluctuations of the line: these should grow like the distance to the power $\frac{1}{2}$ on length scales less than ξ , and to the power $\frac{1}{3}$ on larger distances on length scales between ξ and L_c . More recently, Kardar and Ertaz [11] have performed a dynamic renormalization group calculation for the contact-line at zero temperature, subject to a uniform pulling force, and also find a roughness exponent $\frac{1}{3}$. These scaling laws have been confirmed in recent experiments on the wetting of helium on a caesium substrate [4], confirming the validity of the collective pinning picture in this case.

The aim of our paper is to go beyond the scaling analysis and provide a quantitative computation of the correlation function of the line, on length scales smaller than L_c . We use the replica method together with a Gaussian variational approximation, with replica symmetry breaking [12]. This approach, which is exact in the limit of large dimensions, has been shown to predict the correct wandering exponents for a

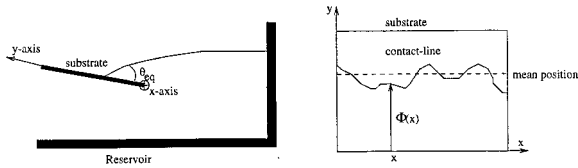


FIG. 1. Sketch of the experimental setup.

random field type of disorder, but not for one-dimensional random bond systems [12]. Apart from the exponent itself, it has been shown to give good quantitative results even for zero-dimensional random field systems [13–15]. We will show that this method, when applied to the contact line problem, confirms the scaling exponents derived before, but also provides the prefactor and a full description of the crossover between the two regimes around the Larkin length. Note that in the case of random bond systems, the exponents given by the replica method are only approximate.

The paper is organized as follows. We introduce the model in Sec. II. In Sec. III, we present for completeness a scaling argument which gives the roughness exponents, and we obtain an expression for the Larkin length by a perturbative approach. In Sec. IV, we present the replica calculation and compute within a variational approximation the full correlation function in the limit of low temperatures. In Sec. V, we compare our theoretical prediction with experimental data.

II. THE MODEL

Consider a situation given by Fig. 1, where the liquid wets an impure substrate which is slightly inclined with respect to the horizontal. We denote by (x, y) the space coordinates of the substrate. The excess energy per unit area due to pinning is given by

$$e(x, y) = \gamma_{sl}(x, y) - \gamma_{sv}(x, y) - \overline{\gamma_{sl}(x, y) - \gamma_{sv}(x, y)} \quad (2)$$

resulting in a total pinning energy

$$\int_0^L dx \int_0^{\Phi(x)} dy e(x, y), \quad (3)$$

where $\Phi(x)$ is the height of the the contact line at the abscissa x , and L is the width of the substrate. As for the pinning energy per unit area or force per unit length $e(x, y)$, we shall suppose that it is Gaussian distributed of mean zero, which is the case if it results from a large number of microscopic interactions, and that it has local correlations on length scales of order Δ . Specifically, we choose

$$\overline{e(x, y)e(x', y')} = \frac{W}{\Delta^2} \delta(x - x') C\left(\left|\frac{y - y'}{\Delta}\right|\right), \quad (4)$$

where the correlation function $C(r)$ is normalized to $C(0) = 1$ and $C''(0) = 1/\Delta^2$, and decreases fast enough to zero for $r \gg 1$. The asymmetry introduced in Eq. (4) between the two directions x and y is for computational convenience. In most physical situations, the distribution of disorder should be isotropic in the x - y plane, leading to a correlation in the x direction on length scales of order Δ . We believe, however, that this correlation is irrelevant: coarse-graining the force in

the x direction on scales of order Δ leads to a discretized (in x) version of Eq. (4), which is equivalent to the form which we use (with a cutoff in small x length scales, of order Δ). As for the shape of the function $C(r)$, we shall first use

$$C(r) = f(r) = \exp(-r^2/2). \quad (5)$$

We must also add to the random potential term a capillary energy term, which, if we neglect gravity and suppose that the slope of the liquid-vapor interface varies smoothly, is given by

$$E_{\text{cap}} = \frac{c}{2} \int_{2\pi/L \leq |k| \leq 2\pi/\Delta} \frac{dk}{2\pi} |k| |\Phi(k)|^2 \quad (6)$$

with $c = \gamma \sin^2 \theta_{\text{eq}}/2$ [9], θ_{eq} being the average equilibrium contact angle. The final Hamiltonian is thus

$$H = \frac{c}{2} \int_{2\pi/L \leq |k| \leq 2\pi/\Delta} \frac{dk}{2\pi} |k| |\Phi(k)|^2 + \int_0^L dx V(x, \Phi(x)), \quad (7)$$

where $V(x, \Phi) = \int_0^{\Phi(x)} dy e(x, y)$. As a sum of independent Gaussian variables, $V(x, \Phi)$ is a Gaussian variable of mean zero, and up to a uniform arbitrary random shift we can choose

$$\overline{V(x, \Phi)V(x', \Phi')} = -W \delta(x - x') f\left(\left(\frac{\Phi - \Phi'}{\Delta}\right)^2\right), \quad (8)$$

where $f(u)$ is a function which grows as $\sqrt{|u|}$ for large $|u|$. Its precise form depends on the correlation function C of the energy per unit area, and is given in the simple case (5) by

$$f(u^2) = |u| \int_0^{|u|} dv e^{-v^2/2} - (1 - e^{-u^2/2}). \quad (9)$$

Note that V is a long-ranged potential and for $|u| \gg 1$, $f(u) \sim \sqrt{|u|}$.

This model is probably a good model for the problem of a contact line on a disordered substrate under the following hypotheses.

(i) The slope of the liquid-vapor interface is everywhere small. This allows us to expand the surface energy term $\sqrt{1 + (\nabla \zeta)^2}$, where ζ is the position of the liquid-vapor interface.

(ii) The length of the contact line is small compared with the capillary length, so that one can neglect gravity. In the geometry considered, the effective capillary length is given by $\sqrt{\gamma/\rho g \sin \alpha}$, where α is the tilt angle of the substrate with respect to horizontal [4].

(iii) The defects in the substrate are weak and give rise to collective pinning.

III. PERTURBATION THEORY AND SCALING ARGUMENTS

For completeness we rederive in this section an expression for the Larkin length by perturbation theory, and review the scaling derivation of the roughness exponents.

A. The Larkin length

On a sufficiently small length scale, we can assume that the difference in heights between any two points is small compared with the correlation length Δ of the potential. We can thus linearize the potential term [6] such that $V(x, \Phi(x)) \approx V(x, 0) - e(x)\Phi(x)$. This leads to a random force problem with a force correlation function $\overline{e(x)e(x')} = (W/\Delta^2)\delta(x-x')$. Rewriting the Hamiltonian as

$$H = \frac{c}{2} \int \frac{dk}{2\pi} |k| \left| \Phi(k) - \frac{e(k)}{c|k|} \right|^2 - \frac{1}{2c} \int \frac{dk}{2\pi} \frac{|e(k)|^2}{|k|}, \quad (10)$$

we get for $T \rightarrow 0$ and $\Delta \ll |x-x'| \ll L$

$$\begin{aligned} \overline{[\Phi(x) - \Phi(x')]^2} &= \frac{2W}{c^2\Delta^2} \int \frac{dk}{2\pi} \frac{\{1 - \cos[k(x-x')]\}}{k^2} \\ &= \frac{W}{c^2\Delta^2} |x-x'|. \end{aligned} \quad (11)$$

Throughout the paper, we denote thermal averages by angular brackets and the average over disorder by an overbar. The linear approximation is no longer valid when $|\Phi(x) - \Phi(x')|$ becomes of the order Δ . Typically $|x-x'|$ is then of order $\xi = c^2\Delta^4/W$, where ξ is the so-called Larkin length. The critical exponent in the Larkin regime is given by $\frac{1}{2}$.

B. Roughness exponent for large fluctuations

On length scales larger than ξ , the fluctuations of the line are greater than the correlation length Δ and perturbation theory breaks down. One can estimate the wandering exponent by a simple scaling argument as follows [12]. The Hamiltonian is given by Eq. (7) and we can no longer linearize the potential term in Eq. (7).

We consider the scale transformation, $x \rightarrow lx$, $\Phi(x) \rightarrow l^\zeta \Phi(x)$, $V(x, \Phi(x)) \rightarrow l^\lambda V(x, \Phi(x))$. Imposing that the two terms in the Hamiltonian scale in the same way and that the potential term keeps the same statistics after rescaling, we have

$$\lambda = 2\zeta - 1 \quad \text{and} \quad 2\lambda = -1 + \zeta \quad (12)$$

and so $\zeta = \frac{1}{3}$. Note that this is less than $\frac{1}{2}$, which is the value of the exponent in the Larkin regime. This is not surprising since on a still larger length scale (larger than the capillary length) we expect the line to be flat and $\zeta = 0$.

This exponent can be recovered by the following Imry-Ma argument [1, 8–10]. On a scale L , the line fluctuates over a distance Φ . The elastic energy contribution then scales as $c\Phi^2$. As for the pinning energy, since it is a sum of independent Gaussian variables, it scales as $\sqrt{W\Delta}\sqrt{L\Phi}/\Delta^2$, where $\sqrt{W\Delta}$ is a measure of the pinning energy on an area Δ^2 and $L\Phi/\Delta^2$ is an order of magnitude of the number of such pinning sites. Minimizing the total energy $c\Phi^2 - \sqrt{W\Delta}\sqrt{L\Phi}/\Delta^2$ with respect to Φ , we get $\Phi \approx \Delta(L/\xi)^{1/3}$ with $\xi \sim c^2\Delta^4/W$.

IV. THE REPLICA COMPUTATION

A. Computation of the free energy

We now turn to a microscopic computation of the free energy $F = -T \ln Z$. Since the self-energy is a self-averaging quantity, the typical free energy is equal to the average of F over the disorder. We compute it from the replica method with an analytic continuation of Z^n , for $n \rightarrow 0$ [16]. The n th power of the partition function

$$\begin{aligned} Z^n &= \int \prod_{a=1}^n d[\Phi_a] \exp \left\{ -\frac{\beta c}{2} \int \frac{dk}{2\pi} \sum_a |k| |\Phi_a(k)|^2 \right. \\ &\quad \left. - \beta \sum_a \int_0^L dx V(x, \Phi_a(x)) \right\} \end{aligned} \quad (13)$$

gives after averaging over the disorder

$$\overline{Z^n} = \int \prod_{a=1}^n d[\Phi_a] \exp \{ -\beta \mathcal{H}_n[\Phi_a] \}, \quad (14)$$

where

$$\begin{aligned} \mathcal{H}_n &= \frac{c}{2} \int \frac{dk}{2\pi} \sum_a |k| |\Phi_a(k)|^2 \\ &\quad + \frac{\beta W}{2} \sum_{a,b} \int_0^L dx f \left[\left(\frac{\Phi_a(x) - \Phi_b(x)}{\Delta} \right)^2 \right]. \end{aligned} \quad (15)$$

We note that the expression of the free energy is invariant with respect to a translation of the center of mass of the line $\Phi_{\text{CM}} = 1/L \int_0^L dx \Phi(x) = (1/L)\Phi(k=0)$. We can fix the center of mass so that there is no integration on the $k=0$ mode. The partition function $\overline{Z^n}$ cannot be computed directly. Following [12], we perform a variational calculation based on the variational Hamiltonian

$$\mathcal{H}_0 = \int \frac{dk}{2\pi} \sum_{a,b=1}^n \Phi_a(-k) G_{ab}^{-1}(k) \Phi_b(k), \quad (16)$$

where G^{-1} is a hierarchical Parisi matrix.

The variational free energy

$$\mathcal{F} = \frac{-1}{\beta n} \ln Z_0 + \frac{1}{n} \langle \mathcal{H}_n - \mathcal{H}_0 \rangle_0 \quad (17)$$

gives up to a constant term,

$$\begin{aligned} \frac{\mathcal{F}}{L} &= \lim_{n \rightarrow 0} \frac{1}{n} \left[\frac{-1}{2\beta} \int \frac{dk}{2\pi} \text{Tr}_a \ln G + \frac{c}{2\beta} \int \frac{dk}{2\pi} |k| \sum_a G_{aa}(k) \right. \\ &\quad \left. + \frac{\beta W}{2} \sum_{a \neq b} \hat{f} \left(\frac{B_{ab}}{\Delta^2} \right) \right], \end{aligned} \quad (18)$$

where

$$\hat{f}(z) = \int_{-\infty}^{\infty} \frac{du}{\sqrt{2\pi}} f(u^2 z) e^{-u^2/2} = \sqrt{1+z} - 1 \quad (19)$$

and

$$B_{ab} = \frac{1}{\beta} \int \frac{dk}{2\pi} [G_{aa}(k) + G_{bb}(k) - 2G_{ab}(k)]. \quad (20)$$

The optimal free energy is obtained for a matrix G verifying the stationarity conditions $\partial \mathcal{F} / \partial G_{ab} = 0$, which read

$$G_{ab}^{-1} = \frac{-2\beta W}{\Delta^2} \hat{f}' \left(\frac{B_{ab}}{\Delta^2} \right) \quad \text{for } a \neq b, \quad (21)$$

$$\sum_b G_{ab}^{-1} = c|k|.$$

More details on this approach can be found in [12,16,17].

B. The replica symmetry breaking solution

To solve Eqs. (21), we suppose that the matrix G has a hierarchical replica symmetry breaking structure in the manner of Parisi. We can write $G_{ab}^{-1} = (c|k| - \bar{\sigma}) \delta_{ab} - \sigma_{ab}$. G^{-1} is thus parametrized by a diagonal part $c|k| - \bar{\sigma}$, and a function $\sigma(u)$ defined on the interval $[0,1]$. [From Eqs. (21), we know that the off-diagonal elements of G^{-1} do not depend on k .] The optimization equations for G can then be written as

$$\sigma(u) = \frac{2\beta W}{\Delta^2} \hat{f}' \left(\frac{B(u)}{\Delta^2} \right) \quad (22)$$

with

$$B(u) = \frac{2}{\beta} \int \frac{dk}{2\pi} [\bar{g}(k) - g(k, u)]. \quad (23)$$

The solution to these equations is described in Appendix A. It is best written in terms of the function

$$[\sigma](u) = u\sigma(u) - \int_0^u dv \sigma(v) \quad (24)$$

which is given by

$$[\sigma](u) = \frac{W}{\pi c \Delta^4} \left(\frac{u}{u_c} \right)^{3/2} \quad \text{for } u \leq u_c, \quad (25)$$

$$[\sigma](u) = \frac{W}{\pi c \Delta^4} \quad \text{for } u \geq u_c,$$

with

$$u_c \approx \frac{3T}{\pi c \Delta^2} = \frac{T}{T_c}.$$

The expression for u_c is given by T/T_c for T small compared with T_c . From the expression

$$G_{aa}(k) = \frac{1}{c|k|} \left[1 + \int_0^1 \frac{du}{u^2} \frac{[\sigma](u)}{[\sigma](u) + c|k|} \right] \quad (26)$$

we get for $T \rightarrow 0$,

$$\left| \frac{x-x'}{\Delta} \right| \gg 1 \quad \text{and} \quad \left| \frac{x-x'}{L} \right| \ll 1, \quad (27)$$

$$\sqrt{\langle [\Phi(x) - \Phi(x')]^2 \rangle} = \Delta \mathcal{H} \left(\frac{x-x'}{\xi} \right),$$

where

$$\mathcal{H}^2(x) = \frac{4}{3} \left(\frac{x}{\pi} \right)^{2/3} \int_0^\infty dk \frac{[1 - \cos(k)]}{k^{5/3}} \int_0^{(x/\pi k)^{1/3}} \frac{dw}{w^3 + 1}$$

$$+ \frac{2x}{3\pi} \int_0^\infty dk \frac{[1 - \cos(k)]}{k(x/\pi + k)} \quad (28)$$

and $\xi = c^2 \Delta^4 / W$.

The function \mathcal{H} has the following asymptotic behavior. For small x , $\mathcal{H}(x) \approx \sqrt{|x|}$ and for large x , $\mathcal{H}(x) \approx 1.14|x|^{1/3}$.

When $|x-x'| \leq \xi$,

$$\sqrt{\langle [\Phi(x) - \Phi(x')]^2 \rangle} \approx \Delta \left| \frac{x-x'}{\xi} \right|^{1/2}. \quad (29)$$

When $|x-x'| \geq \xi$,

$$\sqrt{\langle [\Phi(x) - \Phi(x')]^2 \rangle} \approx 1.14 \Delta \left| \frac{x-x'}{\xi} \right|^{1/3}. \quad (30)$$

C. A more general form of the disorder

We can show that even in the more general case where we only impose that the correlation function of the potential has the asymptotic behavior $f(|u|) \sim \sqrt{|u|}$ for large $|u|$, the height correlation function can be put in the form

$$\sqrt{\langle [\Phi(x) - \Phi(x')]^2 \rangle} = \Delta \mathcal{G} \left(\frac{x-x'}{\xi} \right) \quad (31)$$

in the limit $T \rightarrow 0$, and for $\Delta \ll |x-x'| \leq L$. The derivation of \mathcal{G} is given in Appendix B. \mathcal{G} depends on a function h , where the inverse of h is given by $h^{-1}(x) = f'''(x)/f''(x)$.

D. Effect of the cutoff Δ

On scales comparable to Δ , there are corrections to Eq. (28). When we take into account the cutoff Δ , \mathcal{H} is replaced by

$$\mathcal{H}_1^2(x, \lambda) = \frac{4}{3} \left(\frac{x}{\pi} \right)^{2/3} \int_0^{2\pi\lambda x} \frac{dk}{k^{5/3}} [1 - \cos(k)] \int_0^{(x/\pi k)^{1/3}} \frac{dw}{w^3 + 1}$$

$$+ \frac{2x}{3\pi} \int_0^{2\pi\lambda x} \frac{dk}{k(x/\pi + k)} [1 - \cos(k)], \quad (32)$$

where $\lambda = \xi/\Delta$. The effect of the cutoff is to shift the theoretical curve slightly downwards, especially in the region of small x .

E. Effect of gravity

To take into account gravity, we must replace the kernel $|k|$ in the Hamiltonian (7) by $\sqrt{k^2 + \mu^2}$, with $\mu = 1/L_c$, where

L_c is the capillary length. Generalizing the previous calculations, we can express $[\sigma](u)$ in terms of an inverse function \mathcal{I}^{-1} . When the Larkin length is sufficiently small compared with the capillary length, we have in the limit where $T \ll T_c$

$$\begin{aligned} [\sigma](u) &= 0 \quad \text{for } u \leq u_1, \\ [\sigma](u) &= \mu c \mathcal{I}^{-1} \left[\frac{L_c}{\pi \xi} \left(\frac{u}{u_c} \right)^{3/2} \right] \quad \text{for } u_1 \leq u \leq u'_c, \quad (33) \\ [\sigma](u) &= \mu c \mathcal{I}^{-1} \left[\frac{L_c}{\pi \xi} \left(\frac{u'_c}{u_c} \right)^{3/2} \right] \quad \text{for } u \geq u'_c, \end{aligned}$$

with

$$u_1 = u_c \left(\frac{\pi \xi}{L_c} \mathcal{I}(0) \right)^{2/3} \quad \text{and} \quad u_c \approx \frac{T}{T_c}.$$

As for u'_c , it is slightly larger than u_c and also of order T/T_c . A more detailed description is provided in Appendix C. When the capillary length goes to infinity, u_1 tends towards 0 and u'_c towards u_c . The function $\mathcal{I}(x)$ is given by

$$\mathcal{I}(x) = \left(\int_0^\infty \frac{dk}{(\sqrt{q^2+1+x})^2} \right)^2 \left(2 \int_0^\infty \frac{dk}{(\sqrt{q^2+1+x})^3} \right)^{-3/2} \quad (34)$$

and for large x , $\mathcal{I}(x) \approx x$. This asymptotic behavior ensures that we do recover the results of Sec. V when μ goes to zero. The correlation is then given by

$$\sqrt{\langle [\Phi(x) - \Phi(x')]^2 \rangle} = \Delta \mathcal{H}_g \left(\frac{x-x'}{\xi}, \frac{\pi \xi}{L_c} \right), \quad (35)$$

where

$$\begin{aligned} \mathcal{H}_g^2(x, \lambda) &= \frac{4}{3} \int_0^\infty dk \frac{1 - \cos(kx/\pi)}{\sqrt{k^2 + \lambda^2}} \int_{[\lambda \mathcal{I}(0)]^{1/3}}^{(u'_c/u_c)^{1/2}} dw \frac{\lambda \mathcal{I}^{-1}(w^3/\lambda)}{\lambda \mathcal{I}^{-1}(w^3/\lambda) + \sqrt{k^2 + \lambda^2}} \\ &+ \frac{2}{3} \frac{u_c}{u'_c} \int_0^\infty dk \frac{1 - \cos(kx/\pi)}{\sqrt{k^2 + \lambda^2}} \frac{\lambda \mathcal{I}^{-1}(1/\lambda)}{\lambda \mathcal{I}^{-1}(1/\lambda) + \sqrt{k^2 + \lambda^2}}. \quad (36) \end{aligned}$$

The asymptotic behavior of \mathcal{H}_g is different from that of \mathcal{H} . For small x ,

$$\begin{aligned} \mathcal{H}_g^2(x, \lambda) &\approx x \left\{ \frac{2}{3} \int_{[\lambda \mathcal{I}(0)]^{1/3}}^{(u'_c/u_c)^{1/2}} dw \frac{\lambda}{w^3} \mathcal{I}^{-1}(w^3/\lambda) \right. \\ &\left. + \frac{u_c}{3u'_c} \lambda \mathcal{I}^{-1}(1/\lambda) \right\} \quad (37) \end{aligned}$$

and for large x , $\mathcal{H}_g(x, \lambda)$ tends towards a constant depending on λ .

From the previous equations we can see that gravity has a significant effect when $\pi \xi/L_c$ becomes of order 1, where ξ is the Larkin length and L_c is the capillary length. Moreover, we can also note that the correction for small λ to the case without gravity is of order $\lambda^{1/3}$. The limit λ going to 0 is thus a rather slow one.

V. COMPARISON WITH EXPERIMENT

A. The experimental setup

We have fitted the data from experiments carried out by Guthmann and Rolley [4] with our theoretical curve. The experiments study the wetting properties of liquid helium 4 on caesium below the wetting transition temperature which is about 2 K. Above that temperature, caesium is wetted by helium. In the experiments carried out by Guthmann and Rolley, the substrate consists of caesium deposited on a gold mirror which is slightly inclined with respect to the horizontal (see Fig. 1). The wetted defects are small areas on the substrate where the caesium has been oxidized. The experi-

ments are carried out on a range of temperatures going from about 1 K to 2 K. There is a constant inflow of helium at the bottom of the helium reservoir to maintain the contact angle to its maximum value θ_a , the advancing angle, which is in general different from the equilibrium contact angle θ_{eq} (see Fig. 1). This is necessary because otherwise the liquid would recede and the contact angle would shrink to zero due to strong hysteresis. Height correlations are calculated from snapshots of the advancing line when it is pinned. The incoming helium is regulated to ensure that the line moves with a small velocity and so we can probably suppose that we are just at the limit of depinning each time the line is pinned. While the experiments thus involve a line which is moving very slowly, our theory is a static theory which assumes equilibrium. It is not clear *a priori* that it can apply to the experimental situation, but as we shall see, the quality of the agreement (together with the lack of more quantitative theoretical results on out-of-equilibrium dynamics) justifies it *a posteriori*. The predicted order of magnitude of T_c given by Eq. (25) is $c\Delta^2 = \gamma \sin^2(\theta_{\text{eq}}) \Delta^2/2$. The size of the impurities can be measured experimentally and is of the order of 20 μm . We thus expect the correlation length to be a few times this size. For temperatures not too close to transition temperature, $\theta_{\text{eq}} \sim 20^\circ$ and $\gamma \sim 10^{19} \text{ Km}^{-2}$. This leads to a typical estimate $T_c \sim 10^5 \text{ K}$, in the experimental conditions of [4]. Therefore, T/T_c is of order 10^{-5} and the system is effectively at low temperatures, justifying the low-temperature limit in our computations. This effect is due to the fact that the defects have a range of at most a hundred micrometers: this had been already pointed out in [7].

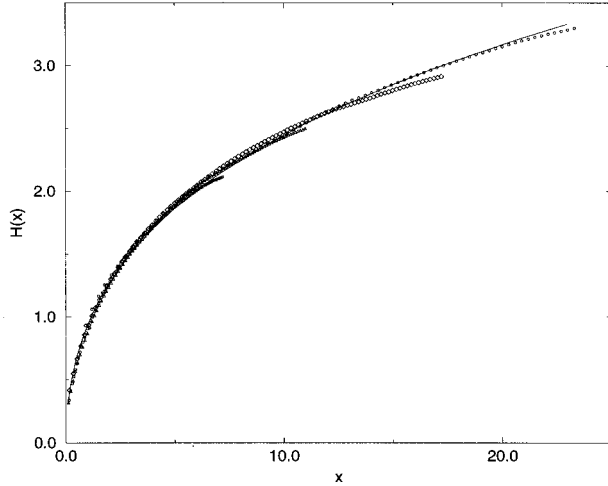


FIG. 2. We rescale the experimental curves on the theoretical curve \mathcal{H} for the case without gravity. The circles represent the data for the temperature $T=1.93$ K, the diamonds $T=1.9$ K, the triangles $T=1.8$ K, and the squares $T=1.72$ K.

B. Comparison between experimental data and the theory for a Gaussian correlation function of the disorder

We consider experimental data for height correlations \mathcal{H} for temperatures $T=1.72, 1.8, 1.9,$ and 1.93 K. The equilibrium angle θ_{eq} , the liquid-vapor interfacial tension γ , and the ‘‘potential strength’’ W depend on the temperature, and so the various experimental curves correspond *a priori* to different values of the Larkin length. Instead, the correlation length Δ which depends only on the substrate is expected to remain constant. We have thus fitted the experimental curves to the theoretical prediction (27) and (35), with the same Δ but different ξ 's.

We proceed as follows. Neglecting gravity, we first minimize the error function

$$\frac{1}{\sum_j N_j} \sum_{j=1}^4 \sum_{i=1}^{N_j} [\Delta \mathcal{H}(x_i/\xi_j) - \mathcal{H}_{\text{exp}}(x_i)]^2 \quad (38)$$

with respect to Δ and ξ_j for $j \in [1,4]$, where j denotes a given experimental curve at the temperature T_j , x_i are the experimental points, N_j is the number of points of curve j , and ξ_j is the correlation length at temperature T_j . This procedure yields $\Delta = 18 \mu\text{m}$. In Fig. 2, we fit each experimental curve on the theoretical curve \mathcal{H} . We rescale each experimental curve by the corresponding $1/\xi$ in the x direction and by $1/\Delta$ in the y direction. In the table below, we give the values of ξ_j and the ratios ξ_j/ξ_1 , where ξ_1 is the correlation length at the highest temperature, for $\Delta \approx 18 \mu\text{m}$. In Fig. 3, we rescale the theoretical curve on each of the experimental curves by the corresponding ξ in the x direction and by Δ in the y direction. The axes are in μm .

T (K)	=	1.72	1.8	1.9	1.93	
ξ (μm)	\approx	220	145	92	53	
ξ/ξ_1	\approx	4.1	2.7	1.7	1	(39)

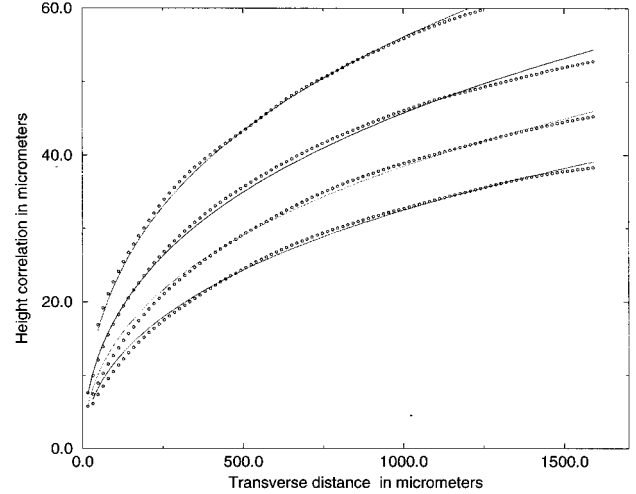


FIG. 3. We have rescaled the theoretical curve \mathcal{H} in the absence of gravity on the experimental curves by the same amount Δ in the y direction and by different amounts ξ in the x direction. On the x axis, we have represented the distance in μm between two points on the line, and on the y axis the average height difference between them. The circles represent the experimental data. From top to bottom, we go from 1.93 K, to 1.9 K, 1.8 K, and to 1.72 K.

The dependence of ξ on the temperature is related to the variations of W , γ , and θ_{eq} , which are not known well enough for a detailed comparison. In Fig. 3, we note that each of the rescaled experimental curve departs from the theoretical curve after some time. Moreover, we note that the general tendency is that the experimental curves have a slightly larger curvature than the rescaled theoretical curve. This is an indication that gravity could indeed play a significant part. Indeed, the effective capillary length in the experimental conditions is of the order 2 mm, and experimentally the correlations are measured for distances up to about 1.5 mm, which is actually not small compared with the capillary length.

To check whether gravity does or does not have a significant effect, we have recommenced the previous steps with \mathcal{H}_g instead of \mathcal{H} . The capillary length L_c can be calculated for the different temperatures from the experimental measurements of γ . We now minimize the error function

$$\frac{1}{\sum_j N_j} \sum_{j=1}^4 \sum_{i=1}^{N_j} [\Delta \mathcal{H}_g(x_i/\xi_j, \pi \xi_j/L_c) - \mathcal{H}_{\text{exp}}(x_i)]^2. \quad (40)$$

We find very different values for the parameters. In this case, $\Delta \approx 75 \mu\text{m}$. In the table below, we indicate the values of the capillary lengths and Larkin lengths for the different temperatures,

T (K)	=	1.72	1.8	1.9	1.93	
L_c (μm)	\approx	1855	1838	1819	1823	
ξ (μm)	\approx	477	422	362	295.	(41)

In Fig. 4, we fit the experimental curves on the corresponding theoretical curve $\mathcal{H}_g(x, \lambda)$. The fit is clearly better at

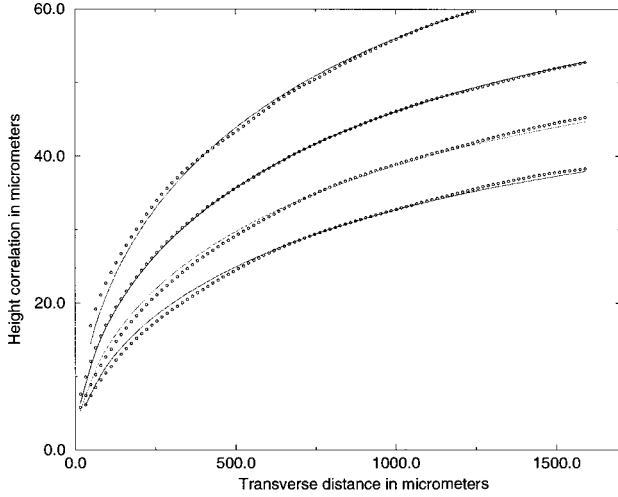


FIG. 4. We rescale the theoretical curve \mathcal{H}_g on the different experimental curves. The axes are the same as for Fig. 3. The upper curve corresponds to the highest temperature and the lowest curve to the lowest temperature.

large x in this case since we have gotten rid of the systematic drift from the theory for large fluctuations.

Since gravity is present in the experiment, it must be included in the analysis. What we find is that, as the length scales which are probed become comparable to the capillary length, the inclusion of gravity in the analysis modifies quite a bit the results of the fit. It is not so surprising that the theory without gravity could give a reasonable fit since it predicted the exponents correctly, but it gave a poor result for the Larkin length. In general, the correlation length will depend quite a lot on the precise form of the disorder, but one can expect it to be a few times the size of the impurities, so that our result $\Delta = 75 \mu\text{m}$ is indeed compatible with the estimated impurity size in the experiment. A better experimental control of the type and size of the impurities would be needed in order to really check this point.

VI. DISCUSSION AND PERSPECTIVES

This model for the pinning of a contact line on a disordered substrate fits quite well the experimental data but there are nevertheless a few points that still need to be cleared. For instance, we have supposed that the line is in thermal equilibrium in order to write the usual partition function, and at the end of the calculation we have taken the temperature to be zero since, as we can see from the numerical values of the parameters, the problem is actually a zero-temperature problem. However, in doing so we retain only the states with the lowest energy. Experimentally the correlations are not measured for the ground state of the line but for any state that can be reached dynamically by the experimental procedure. These states could be metastable stable, which does not necessarily have the same statistical properties as the ground state. But as we have seen from the third fit, the fluctuations of the line do not go beyond the correlation length. So even though we are out of the Larkin regime, the fluctuations are still relatively small and this is perhaps an effect of gravity.

ACKNOWLEDGMENTS

It is a pleasure to thank C. Guthmann, A. Prevost, and E. Rolley for several stimulating discussions. We would also like to thank J. P. Bouchaud and J. Vannimenus.

APPENDIX A: COMPUTATION OF THE FUNCTION $[\sigma](u)$

We give in this appendix some details of the calculation of the function $[\sigma](u)$. We have from Sec. IV

$$\sigma(u) = \frac{2\beta W}{\Delta^2} \hat{f}'\left(\frac{B(u)}{\Delta^2}\right), \quad (\text{A1})$$

where

$$B(u) = \frac{2}{\beta} \int \frac{dk}{2\pi} [\bar{g}(k) - g(k, u)] \quad (\text{A2})$$

and from [12]

$$\bar{g}(k) - g(k, u) = \frac{1}{u[c|k| + [\sigma](u)]} \int_u^1 \frac{dv}{v^2} \frac{1}{c|k| + [\sigma](v)}. \quad (\text{A3})$$

Differentiating Eq. (A1) gives

$$\sigma'(u) = \frac{2\beta W}{\Delta^4} B'(u) \hat{f}''\left(\frac{B(u)}{\Delta^2}\right) \quad (\text{A4})$$

and replacing $B'(u)$ in Eq. (A4) by its expression

$$B'(u) = -\frac{2}{\beta\pi c} \frac{\sigma'(u)}{[\sigma](u)} \quad (\text{A5})$$

leads to

$$\sigma'(u) = 0 \quad (\text{A6})$$

or

$$1 = -\frac{4W}{\pi c \Delta^4} \frac{1}{[\sigma](u)} \hat{f}''\left(\frac{B(u)}{\Delta^2}\right).$$

We express $B(u)/\Delta^2$ in terms of $[\sigma](u)$ by inverting the second equation of Eqs. (A6). This gives

$$\hat{f}''^{-1}\left(-\frac{\pi c \Delta^4}{4W} [\sigma](u)\right) = \frac{B(u)}{\Delta^2}. \quad (\text{A7})$$

Differentiating Eq. (A7), and using expression (A4) to express $B'(u)$, and the fact that $[\sigma]'(u) = u\sigma'(u)$, we get

$$\frac{\hat{f}'''}{\hat{f}''}\left(\frac{B(u)}{\Delta^2}\right) = -\frac{\beta\pi c \Delta^2}{2} u = -\frac{3T_c}{2T} u, \quad (\text{A8})$$

where

$$\hat{f}'(x) = \frac{1}{2\sqrt{1+x}}. \quad (\text{A9})$$

From Eqs. (A8) and (A9), we have

$$\frac{B(u)}{\Delta^2} = -1 + \frac{3T}{\pi c u \Delta^2} = -1 + \frac{T}{T_c} \frac{1}{u}. \quad (\text{A10})$$

Multiplying both sides of Eq. (A5) by u , and using Eq. (A10), we get after integrating over u ,

$$[\sigma](u) = A u^{3/2}. \quad (\text{A11})$$

The breakpoint u_c , above which the solutions to Eqs. (A10) and (A11) are no longer valid, is given by

$$B(u_c) = \Delta^2 \left(-1 + \frac{T}{T_c} \frac{1}{u_c} \right) = \frac{2}{3} \frac{T}{T_c} \ln \left(1 + \frac{2\pi c}{\Delta[\sigma](u_c)} \right). \quad (\text{A12})$$

When T/T_c goes to 0, $u_c \approx T/T_c$. Now since $B(u)$ tends to infinity when u tends to 0, we have $\sigma(0) = 0$. For $u \geq u_c$, $B(u) = B(u_c)$ and $[\sigma](u) = [\sigma](u_c)$. To obtain A , we can differentiate Eq. (A12) and compare the result with the expression for $\sigma'(u)$. We find $A = (W/\pi c \Delta^4)(1/u_c^{3/2})$. For $u \geq u_c$, $\sigma'(u) = 0$ and so $[\sigma](u) = [\sigma](u_c) = W/\pi c \Delta^4$.

APPENDIX B: GENERAL FORM OF THE CORRELATION FUNCTION FOR ARBITRARY DISORDER

In this appendix we derive the height correlation function for a more general form of the function f appearing in the correlation function of the disorder (8). We only impose that $f(|u|) \sim \lambda \sqrt{|u|}$ for large u , where λ is some constant, such that $\hat{f}(u) \sim \sqrt{|u|}$. We shall keep the same notations as in Appendix A. In this more general case, Eqs. (A1), (A5), and (A8) from Appendix A are still valid. We define the function h^{-1} for positive x as

$$h^{-1}(x) = \frac{\hat{f}'''(x)}{\hat{f}''(x)}, \quad (\text{B1})$$

where $h^{-1}(x) \sim -3/2x$ for large x . The asymptotic behavior of $h(y)$ for small and negative y is then $-3/2y$. We now express $B(u)$ in terms of h , from Eqs. (A8) and (B1). This gives

$$B(u) = \Delta^2 h \left(-\frac{\pi c \Delta^2}{2T} u \right). \quad (\text{B2})$$

Differentiating the previous equation (B2) gives

$$B'(u) = -\frac{\pi c \Delta^4}{2T} h' \left(-\frac{\pi c \Delta^2}{2T} u \right) \quad (\text{B3})$$

which can be rewritten as

$$\frac{2T}{3T_c} \frac{d}{du} \log[\sigma](u) = w h'(-w) \quad (\text{B4})$$

where $w = (\pi c \Delta^2/2T)u$. Integrating Eq. (B4) gives

$$[\sigma](u) = [\sigma](\epsilon) \exp \int_{3\epsilon/2u_c}^{3u/2u_c} dw w h'(-w). \quad (\text{B5})$$

For $\epsilon \ll u \ll u_c$, we can use the asymptotic form of h in Eq. (B5), which then reads

$$[\sigma](u) = [\sigma](\epsilon) \left(\frac{u}{\epsilon} \right)^{3/2}. \quad (\text{B6})$$

Now for small u , Eq. (A4) becomes in this case

$$\sigma'(u) = \frac{3}{2} \frac{W}{\pi c \Delta^4} \left(\frac{T_c}{T} \right)^{3/2} \frac{1}{\sqrt{u}} \quad (\text{B7})$$

and so for small u , since $[\sigma](0) = 0$, we get

$$[\sigma](u) = \frac{W}{\pi c \Delta^4} \left(\frac{u}{u_c} \right)^{3/2}. \quad (\text{B8})$$

A comparison of this last expression with Eq. (B6) gives

$$[\sigma](\epsilon) = \frac{W}{\pi c \Delta^4} \left(\frac{\epsilon}{u_c} \right)^{3/2}. \quad (\text{B9})$$

Replacing this last expression in Eq. (B5) and taking ϵ to zero leads to

$$[\sigma](u) = \frac{W}{\pi c \Delta^4} \mathcal{S}(u), \quad (\text{B10})$$

where

$$\mathcal{S}(u) = \left(\frac{u}{u_c} \right)^{3/2} \exp \int_0^{3u/2u_c} dw w \left(h'(-w) - \frac{3}{2w^2} \right). \quad (\text{B11})$$

For the sake of simplicity, we will suppose that in this case the break-point up to which expression (B11) is valid, is also u_c in the limit of low temperatures. This implicitly requires that $h(-3/2) = 0$. Then for $u \geq u_c$,

$$\mathcal{S}(u) = \mathcal{S}(u_c) = \exp \int_0^{3/2} dw w \left(h'(-w) - \frac{3}{2w^2} \right). \quad (\text{B12})$$

When \hat{f}' has the simple form (A9), $h'(-w) = 3/2w^2$, and we recover the expression of $[\sigma](u)$ derived in Appendix A. In the limit of low temperatures and for $\Delta \ll |x - x'| \ll L$, the height correlation function is given by

$$\sqrt{\langle [\Phi(x) - \Phi(x')]^2 \rangle} = \Delta \mathcal{G} \left(\frac{x - x'}{\xi} \right) \quad (\text{B13})$$

with

$$\mathcal{G}^2(x) = \frac{4}{3} \left(\frac{x}{\pi} \right)^{2/3} \int_0^\infty dk \frac{[1 - \cos(k)]}{k^{5/3}} \int_0^{(x/\pi k)^{1/3}} dv \frac{1}{v^3 + \exp\left(-\int_0^3 v^{2/2} (\pi k/x)^{2/3} dw \left[h'(-w) - \frac{3}{2w^2} \right]\right)}$$

$$+ \frac{2x}{3\pi} \int_0^\infty dk \frac{[1 - \cos(k)]}{k \left\{ x/\pi + k \exp\left[-\int_0^{3/2} dw \left(h'(-w) - \frac{3}{2w^2} \right)\right] \right\}}. \quad (\text{B14})$$

APPENDIX C: EFFECT OF GRAVITY FOR GIVEN DISORDER

In this appendix, we consider a specific case of the disorder given by Eqs. (8) and (9). To take into account gravity, we must replace the kernel $|k|$ by $\sqrt{|k|^2 + \mu^2}$, with $\mu = 1/L_c$, where L_c is the capillary length. The equations derived in Appendix A are thus no longer valid. If $\sigma'(u)$ is not zero, then Eq. (A7) of Appendix A becomes

$$\frac{B(u)}{\Delta^2} = \hat{f}^{\nu-1} \left(-\frac{\pi c \Delta^4}{4W} \mathcal{K}([\sigma](u)) \right), \quad (\text{C1})$$

where

$$\mathcal{K}(x) = c \mu g \left(\frac{x}{c \mu} \right) \quad (\text{C2})$$

with

$$\frac{1}{g(x)} = \int_0^\infty \frac{dk}{(\sqrt{k^2 + 1} + x)^2}. \quad (\text{C3})$$

Differentiating Eq. (A2) gives

$$B'(u) = -\frac{2\sigma'(u)}{\pi \beta c} \frac{1}{\mathcal{K}([\sigma](u))}. \quad (\text{C4})$$

Differentiating Eq. (C1), and using Eqs. (A4) and (A9), we have

$$1 + \frac{B(u)}{\Delta^2} = \frac{T}{T_c} \frac{1}{u \mathcal{K}'([\sigma](u))}. \quad (\text{C5})$$

Differentiating the previous expression (C5), and using Eq. (C4) we can express $[\sigma](u)$ as

$$\frac{\mathcal{K}([\sigma](u))}{(\mathcal{K}'([\sigma](u)))^{3/2}} = A u^{3/2}, \quad (\text{C6})$$

where A is a constant to be determined. Replacing in Eq. (A4) $B'(u)$ by its expression (C4) and using Eq. (A9) and Eq. (C5) leads to

$$1 = \frac{W}{\pi c \Delta^4} \frac{1}{u_c^{3/2}} \frac{(u \mathcal{K}'([\sigma](u)))^{3/2}}{\mathcal{K}([\sigma](u))}. \quad (\text{C7})$$

Comparing the previous expression with Eq. (C6) gives

$$A = \frac{W}{\pi c \Delta^4} \frac{1}{u_c^{3/2}}. \quad (\text{C8})$$

To express $[\sigma]$, it is convenient to introduce the function \mathcal{I} ,

$$\mathcal{I}(x) = \frac{g(x)}{(g'(x))^{3/2}}, \quad (\text{C9})$$

which is strictly positive and increasing. $\mathcal{I}(0) \approx 0.87$ and $\mathcal{I}(x)$ goes as x when x goes to infinity.

The inverse function \mathcal{I}^{-1} is thus defined on the interval $[\mathcal{I}(0), \infty]$. Since $[\sigma](u)$ must be continuous and $[\sigma](0) = 0$, the function $[\sigma]$ necessarily has a first plateau where $[\sigma](u) = 0$ from $u = 0$ up to a value u_1 given by

$$\mathcal{I}(0) = \frac{W}{\pi c \Delta^4} \frac{1}{\mu c} \left(\frac{u_1}{u_c} \right)^{3/2} = \frac{L_c}{\pi \xi} \left(\frac{u_1}{u_c} \right)^{3/2}. \quad (\text{C10})$$

For $u_1 \leq u \leq u'_c$, where u'_c is the new break point to be determined,

$$[\sigma](u) = c \mu \mathcal{I}^{-1} \left[\frac{L_c}{\pi \xi} \left(\frac{u_1}{u_c} \right)^{3/2} \right]. \quad (\text{C11})$$

The break-point u'_c is obtained using Eqs. (C5) and (A2) is given by

$$\frac{B(u'_c)}{\Delta^2} = -1 + u_c \frac{1}{u'_c \mathcal{K}'([\sigma](u'_c))}$$

$$= \frac{2}{3} u_c \int \frac{dk}{\left(\sqrt{k^2 + 1} + \frac{[\sigma](u'_c)}{\mu c} \right)} \quad (\text{C12})$$

and when T goes to zero

$$u_c \approx u'_c \mathcal{K}'([\sigma](u'_c)) = u'_c g' \left(\frac{[\sigma](u'_c)}{\mu c} \right), \quad (\text{C13})$$

where

$$g'(u) = 2 \int_0^\infty \frac{dq}{(\sqrt{q^2 + 1} + u)^3} \left(\int_0^\infty \frac{dq}{(\sqrt{q^2 + 1} + u)^2} \right)^{-2}. \quad (\text{C14})$$

Since g' is a strictly increasing function, with $g'(0) = 8/\pi^2$ and $g'(\infty) = 1$, in the limit of low temperatures $u_c \leq u'_c \leq u_c/g'(0)$. Since $\mathcal{I}(x)$ is almost linear, we can suppose that $[\sigma](u'_c) \approx W/\pi c \Delta^4 (u'_c/u_c)^{3/2}$ and so Eq. (C13) can be rewritten as

$$\frac{1}{\lambda^{2/3}} = \Omega^{2/3} g'(\Omega) \quad (\text{C15})$$

with

$$\Omega = \frac{1}{\lambda} \left(\frac{u'_c}{u_c} \right)^{3/2} \quad \text{and} \quad \lambda = \frac{\pi \xi}{L_c}. \quad (\text{C16})$$

We can solve for u'_c perturbatively using the solution without gravity. As a first approximation, we can take for λ its value

in the absence of gravity. We can then solve numerically for Ω and for u'_c . For our experimental data, we get by this method $u'_c \approx u_c$. For $u \geq u'_c$, $[\sigma](u) = [\sigma](u'_c)$. The height correlation function is then given by

$$\sqrt{\langle [\Phi(x) - \Phi(x')]^2 \rangle} = \Delta \mathcal{H}_g \left(\frac{x-x'}{\xi}, \frac{\pi \xi}{L_c} \right), \quad (\text{C17})$$

where

$$\begin{aligned} \mathcal{H}_g^2(x, \lambda) = & \frac{4}{3} \int_0^\infty dk \frac{[1 - \cos(kx/\pi)]}{\sqrt{k^2 + \lambda^2}} \int_{[\lambda \mathcal{I}(0)]^{1/3}}^{(\lambda \Omega)^{1/3}} \frac{dw}{w^3} \frac{\lambda \mathcal{I}^{-1}(w^3/\lambda)}{\lambda \mathcal{I}^{-1}(w^3/\lambda) + \sqrt{k^2 + \lambda^2}} \\ & + \frac{2}{3} (\lambda \Omega)^{-2/3} \int_0^\infty dk \frac{[1 - \cos(kx/\pi)]}{\sqrt{k^2 + \lambda^2}} \frac{\lambda \mathcal{I}^{-1}(1/\lambda)}{\lambda \mathcal{I}^{-1}(1/\lambda) + \sqrt{k^2 + \lambda^2}}. \end{aligned} \quad (\text{C18})$$

-
- [1] P. G. de Gennes, *Rev. Mod. Phys.* **57**, 827 (1985).
 [2] G. Forgas, R. Lipowsky, and Th. M. Nieuwenhuizen, in *Phase Transitions and Critical Phenomena*, edited by C. Domb and J. Lebowitz (Academic, New York, 1991).
 [3] T. Halpin-Healy and Y. C. Zhang, *Phys. Rep.* **254**, 215 (1995).
 [4] C. Guthmann, R. Gombrowicz, V. Repain, and E. Rolley, *Phys. Rev. Lett.* **80**, 2865 (1998).
 [5] J. F. Joanny and P. G. de Gennes, *J. Chem. Phys.* **81**, 552 (1984).
 [6] A. I. Larkin, *Zh. Eksp. Teor. Fiz.* **58**, 1466 (1970) [*Sov. Phys. JETP* **31**, 784 (1970)].
 [7] Y. Pomeau and J. Vannimenus, *J. Colloid Interface Sci.* **104**, 477 (1985).
 [8] Y. Imry and S. K. Ma, *Phys. Rev. Lett.* **35**, 1399 (1975).
 [9] M. O. Robbins and J. F. Joanny, *Europhys. Lett.* **3**, 729 (1987).
 [10] D. Huse (unpublished); see Ref. [1], p. 835.
 [11] D. Ertaz and M. Kardar, *Phys. Rev. E* **49**, 2532 (1994).
 [12] M. Mézard and G. Parisi, *J. Phys. I* **1**, 809 (1991).
 [13] A. Engel, *Nucl. Phys. B* **410**, 617 (1993).
 [14] K. Broderix and R. Kree (unpublished).
 [15] M. Mézard and G. Parisi, *J. Phys. I* **2**, 2231 (1992).
 [16] M. Mézard, G. Parisi, and M. Virasoro, *Spin Glass Theory and Beyond* (World Scientific, Singapore, 1987).
 [17] J. P. Bouchaud, M. Mézard, and G. Parisi, *Phys. Rev. E* **52**, 3656 (1995).